Bioresource Technology 337 (2021) 125385

Contents lists available at ScienceDirect

Bioresource Technology

journal homepage: www.elsevier.com/locate/biortech

Carotenoid biosynthetic gene expression, pigment and *n*-3 fatty acid contents in carotenoid-rich *Tetraselmis striata* CTP4 strains under heat stress combined with high light

Lisa M. Schüler [a], Gabriel Bombo [a,b], Paulo Duarte [a], Tamára F. Santos [a], Inês B. Maia [a], Filipa Pinheiro [a], José Marques [a], Rita Jacinto [b], Peter S.C. Schulze [b], Hugo Pereira [b], Luísa Barreira [a,b], João C.S. Varela [a,b,*]

[a] Marine Biotechnology Group, Centre of Marine Sciences, University of Algarve, Campus de Gambelas, 8005-139 Faro, Portugal
[b] Green Colab - Associação Oceano Verde, University of Algarve, Campus de Gambelas, 8005-139 Faro, Portugal

HIGHLIGHTS

- Random mutagenesis coupled with FACS as powerful tool for strain improvement.
- Norflurazon-resistant mutants showed increase in carotenoids and EPA over WT.
- Expression of six carotenogenic genes was upregulated in mutants.
- Mutants showed carotenoid and EPA contents of 10.2 and 4.4 mg g^{-1} DW, respectively.
- Increase in carotenoids and EPA might have improved survival under stress.

GRAPHICAL ABSTRACT

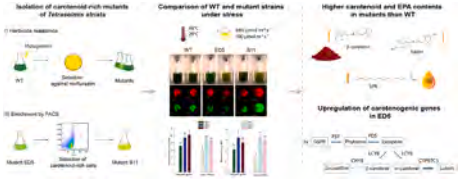

ARTICLE INFO

Keywords:
Microalgae
Random mutagenesis
Flow cytometry
Lutein
EPA

ABSTRACT

In this study, two carotenoid-rich strains of the euryhaline microalga *Tetraselmis striata* CTP4 were isolated by random mutagenesis combined with selection via fluorescence activated cell sorting and growth on norflurazon. Both strains, ED5 and B11, showed an up to 1.5-fold increase in carotenoid contents as compared with the wildtype, independent of the growth conditions. More specifically, violaxanthin, β-carotene and lutein contents reached as high as 1.63, 4.20 and 3.81 mg g^{-1} DW, respectively. Genes coding for phytoene synthase, phytoene desaturase, lycopene-β-cyclase and ε-ring hydroxylase involved in carotenoid biosynthesis were found to be upregulated in ED5 and B11 cells as compared to the wildtype. Both strains showed higher contents of eicosapentaenoic acid as compared with those of the wildtype, reaching up to 4.41 and 2.88 mg g^{-1} DW, respectively. Overall, these results highlight the complexity of changes in carotenoid biosynthesis regulation that are required to improve pigment contents in microalgae.

* Corresponding author.
E-mail address: jvarela@ualg.pt (J.C.S. Varela).

https://doi.org/10.1016/j.biortech.2021.125385
Received 29 April 2021; Received in revised form 2 June 2021; Accepted 3 June 2021
Available online 7 June 2021

1. Introduction

Microalgae are alternative biological feedstocks rich in proteins, carbohydrates, and lipids, containing bioactive high-value compounds such as carotenoids and essential fatty acids. Unlike traditional food crops, microalgae display higher productivities and can grow on non-arable land using non-potable water. Recently, high attention has been paid to microalgae rich in carotenoids and *n*-3 fatty acids, due to their applications in the food, feed, pharmaceutic, nutraceutical and cosmetic industries (Nethravathy et al., 2019). The simultaneous production of several high-value compounds has the potential to decrease production costs and to facilitate the application of the biorefinery concept to microalgal biomass for the manufacture of products with enhanced appeal to stakeholders and consumers alike.

Fatty acids are the major components of lipids, which can be divided into polar and non-polar lipids such as triacylglycerols (TAGs) (Guschina and Harwood, 2013). While TAGs are predominantly composed of saturated fatty acids, polar lipids are structural components of membranes and usually contain high amounts of polyunsaturated fatty acids (PUFA), which play an important role in several defense and signaling mechanisms (Okuyama et al., 2008). For example, under stress conditions, PUFA, e.g., eicosapentaenoic acid (EPA), remove reactive oxygen species (ROS) and thus prevent oxidative stress-induced cell damage. Carotenoids are lipophilic isoprenoid biomolecules and can be divided into two classes, namely carotenes and xanthophylls. The carotenoid biosynthesis in microalgae occurs in the chloroplast and has been explained in detail previously (Mulders et al., 2014; Varela et al., 2015). Briefly, the first carotenoid phytoene results from the condensation of two geranylgeranyl pyrophosphates (GGPP) catalyzed by phytoene synthase (PSY). The following reaction is catalyzed by phytoene desaturase (PDS) leading to lycopene, the branch point of the synthesis. Either β-carotene or α-carotene are synthesized from lycopene depending on the activities of lycopene β- and ε-cyclases (LCYB and LCYE, respectively). The hydroxylation of β-carotene catalyzed by the β-carotene hydroxylase (CHYB) gives rise to the xanthophylls of the violaxanthin cycle. Different types of hydroxylases, namely β-ring hydroxylase CYP97A5 and ε-ring hydroxylase CYP97C3 catalyze the stepwise synthesis of lutein from α-carotene (Kim and DellaPenna, 2006). In the microalgal cell, carotenoids play essential roles in photosynthesis, in light harvesting and energy transfer, as well as in photoprotection by dissipating excess energy as heat, thus preventing photooxidative damage (Mulders et al., 2014). Moreover, xanthophylls such as zeaxanthin are structural components of membranes and may affect the fluidity of the lipid bilayer (Varela et al., 2015). The production of PUFA and carotenoids is not only highly species-dependent but also depends on environmental conditions such as light intensity and temperature. These conditions are known to influence the carotenoid and fatty acid composition in the cell due to changes in enzyme activity, gene expression and other physiological processes (Zhao et al., 2019).

In several attempts at genetic engineering of microalgae to enhance carotenoid and lipid production, one or several biosynthetic genes have been overexpressed, leading to inconsistent results concerning higher carotenoid or lipid levels (Gimpel et al., 2015). This lack of success is most probably due to the existence of several interdependent, rate-limiting enzymatic steps in these complex pathways. Furthermore, specific transformation tools need to be generated for each particular strain, limiting the application of genetic engineering to microalgae. Alternatively, random mutagenesis has been widely used to generate improved strains, a method that does not require prior knowledge of biosynthetic pathways, because no heterologous DNA is introduced in the cell to target specific sequences of the wildtype genome. The combination of mutagenesis with a selection by visual observation or by the use of herbicides has been performed to obtain carotenoid or EPA-rich mutants of several microalgae (Cordero et al., 2011; Huang et al., 2018; Moha-León et al., 2019). For example, the herbicide norflurazon has been shown to not only inhibit PDS but also Δ6 desaturases in microalgae leading to changes in carotenoid and fatty acid composition, respectively (Breitenbach et al., 2001; Cohen and Heimer, 1990). Moreover, fluorescence activated cell sorting (FACS) is a powerful tool to select single cells with desired traits and has been used to enriched strains with higher carotenoid or EPA/lipid contents (Lim et al., 2015; Mendoza et al., 2008; Pereira et al., 2018).

In this study, mutants of a robust, industrial euryhaline microalga *Tetraselmis striata* CTP4 were developed. To this end, random chemical mutagenesis was applied and mutants with improved carotenoid contents were selected using a two-step strategy: i) resistance to the herbicide norflurazon over at least 10 subcultures and ii) enrichment of improved strains by FACS. The carotenoid, chlorophyll, protein, carbohydrate and lipid contents as well as fatty acid profiles of wildtype and mutants were studied under two different growth conditions. Moreover, for the first time in this microalga, the expression profiles of six carotenogenic genes were analyzed. This study provides important information on the regulation of the carotenoid biosynthetic pathway in wildtype and mutant cells of *T. striata*. Furthermore, protein, lipid as well as fatty acid contents were analyzed to better understand the potential of these non-GMO mutants in future products.

2. Materials and methods

2.1. Strain and mesophilic growth conditions

The euryhaline microalga *Tetraselmis striata* CTP4 was isolated from the Ria Formosa, Algarve, Portugal (Pereira et al., 2016). Culture scale-up was performed at mesophilic growth conditions at 20 °C and a light intensity of 100 μmol m^{-2} s^{-1} as reported previously (Pereira et al., 2016; Schulze et al., 2017). Briefly, 50-mL Erlenmeyer flasks containing diluted seawater (20 ppt) enriched with Modified Algal Medium (MAM; Pereira et al., 2016; Schulze et al., 2017) were inoculated with colonies from plates and scaled up to 100-mL test tubes. Growth was followed by optical density measurements at 750 nm and cell count using a Neubauer chamber. Dry weight (DW) was calculated using the following Eq. (1):

$$DW\ \left[g\ L^{-1}\right]\ =\ 1.61\ *\ OD_{750} \quad (1)$$

2.2. Random mutagenesis and mutant selection

Exponentially growing cells of *T. striata* (2×10^6 cells mL^{-1}) were subjected to random mutagenesis by ethyl methane sulfonate (EMS, Merck, USA) as described in Schüler et al. (2020a) with slight modifications. After 10-fold concentration upon centrifugation (3000 *g*, 3 min) and a resuspension in the same media, cells were treated with 100, 150, 200, 250 and 300 mM of EMS for 1 h under mild shaking in the dark. The action of EMS was stopped by addition of sodium thiosulfate to a final concentration of 5% (m/v). Cells were pelleted by centrifugation, washed thrice with sterile seawater (20 ppt) and incubated for 24 h in the dark in fresh media. Afterwards, cells were plated onto solid (agar) MAM plates in serial dilutions and incubated at room temperature (RT) and a light intensity of 100 μmol m^{-2} s^{-1} for 2–3 weeks. Colony forming units were counted to determine cell viability. Mutant selection was carried out by plating at a norflurazon concentration that was otherwise lethal to the wildtype (WT) cells. Herbicide-resistant colonies were subcultured at least 10 times on plates containing norflurazon to confirm their resistance.

2.3. Enrichment of improved strains by fluorescence activated cell sorting (FACS)

Samples of WT and mutant strains with highest carotenoid contents were acquired in a Becton Dickinson FACS Aria II (BD Biosciences, Belgium) equipped with a blue, red and violet laser (488, 633 and 407 nm, respectively) and FACSDiva (version 6.1.3) software. Two filters

were used to record the fluorescence signal, namely FL1 and FL2 centered, respectively, at 695/40 and 530/30 nm after excitation with the blue laser. Cells emitting higher levels of fluorescence due to chlorophyll (FL1) and carotenoids (FL2) were sorted directly onto 96-well microplates containing 250 µL of solid MAM. Plates were incubated at room temperature with a photon flux density of 45 µmol m^{-2} s^{-1} for 3–4 weeks until colonies emerged. Mutants were plated against norflurazon to confirm their resistant phenotype.

2.4. Growth experiment to compare gene expression and biochemical profiles of WT and selected mutants

Pre-cultures of WT, ED5 and B11 strains were grown under mesophilic conditions in 1-L photobioreactors with constant renewal of media to maintain cultures in the exponential growth phase. Afterwards, all strains were inoculated at a biomass concentration of 0.24 g L^{-1} in 1-L bioreactors in triplicate and supplemented with MAM. Cultures were grown under mesophilic (20 °C, 100 µmol m^{-2} s^{-1}) and stress (30 °C, 380 µmol m^{-2} s^{-1}) conditions for three days. Samples for RNA extraction were taken from the inoculum and after one day by centrifugation at the corresponding growth temperature; biomass pellets were immediately frozen in liquid nitrogen and stored at −80 °C until further analysis. Biomass for biochemical analysis was harvested from the inoculum and after two and three days of growth by centrifugation, lyophilized and stored at −20 °C.

2.4.1. Microscopy

After a growth period of three days, images of WT, ED5 and B11 strains were acquired with an Axio Imager Z2 microscope coupled to a Zeiss-Hrm camera (Carl Zeiss Microscopy, Germany) as described previously (Schüler et al., 2020b). Images were treated using Zeiss Zen lite microscope software (BLUE edition 3.3).

2.4.2. RNA extraction and cDNA synthesis

RNA was extracted using the NZYol protocol (NZYTech, Portugal) in combination with RNeasy Mini kit (Qiagen, Germany). To this end, the frozen biomass was resuspended in NZYol and cells were disrupted with glass beads in an MM400 mixer mill (Retsch, Germany) by three cycles at 30 Hz for 1 min with 1 min intervals on ice. The supernatant was collected after centrifugation at 12,000 *g* for 10 min at 4 °C and incubated at room temprature for 7 min, after which 0.2 volumes of chloroform were added, followed by another incubation at room temperature for 3 min. Phase separation was achieved by centrifugation at 12,000 *g* for 15 min at 4 °C and the aqueous upper phase was collected. After the addition of 1 vol of 70% ethanol to the aqueous phase, the solution was transferred to the RNeasy Mini spin column and the manufacturer's instructions were followed. To remove all traces of genomic DNA, on-column DNase digestions using RNase-free DNase sets (Qiagen, Germany) were performed. Extracted RNA was quantified by NanoDrop One spectrophotometry (Thermo Fisher Scientific, USA) and integrity was confirmed by denaturing gel analysis. First strand cDNA synthesis was performed using superscript IV reverse transcriptase (Thermo Fisher Scientific, USA) according to the manufacturer's protocol. A mixture of random hexamers and oligod$(T)_{18}$ primers (1:10) was used and cDNA was synthesized with a prolonged protocol as follows: 23 °C for 10 min, 50 °C for 20 min, 55 °C for 20 min and 65 °C for 10 min. Enzymatic activity was inhibited by incubation at 80 °C for 10 min. The obtained cDNA was diluted 1:50, stored at −20 °C until use in the subsequent reactions.

2.4.3. Primer design and real-time PCR

To identify the sequences of genes involved in carotenoid biosynthesis, *PSY*, *PDS*, *LCYB*, *LCYE*, *CHYB* and *CYP97C3* mRNA sequences of chlorophytes were aligned to the published genome of a related *Tetraselmis striata* strain (AccNo. GCA_006384855.1) using CLC Genomics Workbench 20 (Qiagen, Germany). Upon intron removal, the exon sequences of the aforementioned genes were obtained. Afterwards, primers for real-time PCR were designed using primer-BLAST (NCBI). The primer sequences for the *PDS* and *LCYB* genes were partially adapted from a previous report on *Chlamydomonas* sp., while the primers for *LCYE* were modified from primers targeting the same gene in *Chlorella vulgaris* (Kim et al., 2020; Ma et al., 2019). Transcript expression levels of genes involved in carotenoid biosynthesis were evaluated by amplification using NZYSpeedy qPCR Green Master Mix, ROX plus (NZYTech, Portugal) and a CFX 96-well Real-Time PCR system (BioRad, USA) with the following protocol: initial heating to 95 °C for 2 min, 45 cycles of 95 °C, 5 s, and 62 °C, 20 s (64 °C were used for the primers *CHYB* and *CYP97C3*). Small subunit (*SSU*) 18S ribosomal RNA was used as internal control and raw data were analyzed by the $2^{-\Delta\Delta Ct}$ method based on cycle threshold (Ct) values.

2.4.4. Pigment analysis

Pigment extraction and analysis was performed using samples obtained from the inoculum and after two and three days of growth as described in Schüler et al. (2020a). Briefly, freeze-dried biomass was extracted with methanol using glass bead-based cell disruption. After the recovery of the supernatant, the remaining biomass was reextracted until both the pellet and the supernatant became colorless. The extracts were dried under a gentle nitrogen flow, resuspended in methanol and filtered.

Chlorophyll *a* and *b* contents were determined spectrophotometrically using the following formulae (2 and 3) (Lichtenthaler and Wellburn, 1983):

$$Chla = 15.65\ A_{666} - - 7.34\ A_{653} \quad (2)$$

$$Chlb = 27.05\ A_{653} - - 11.21\ A_{666} \quad (3)$$

Carotenoid profiles were analyzed by an HPLC system equipped with a LiChroCART RP-18 column (5 µm, 250 × 4 mm, LiChrospher) and photodiode-array detector set to 450 nm. For identification and quantification, calibration curves of neoxanthin, violaxanthin, lutein, zeaxanthin and *β*-carotene (Sigma-Aldrich, Portugal) were established.

2.4.5. Biochemical analysis

Biochemical analysis was performed on samples obtained from the inoculum and after three days of growth.

The protein content was determined by CHN elemental analysis using a Vario el III (Vario EL, Elemental Analyzer system, Germany). The final protein content was calculated by multiplying the percentage of nitrogen by 4.78 (Lourenço et al., 2004).

The carbohydrate content was analyzed by the phenol–sulfuric acid method (Dubois et al., 1956). To this end, about 5 mg of freeze-dried biomass was extracted using distilled water and cell disruption by bead-beating in an MM400 mixer mill (Retsch, Germany) at 30 Hz for 5 min. To 1 mL of this aqueous extract an equal amount of 5% (v / v) phenol solution was added and mixed. Afterwards, 5 mL of 67% sulfuric acid was added, mixed and incubated for 10 min at room temperature. The reaction was stopped by incubation on ice for 20 min and the absorbance of the extract was read at 436 nm in a spectrophotometer (PF-12 plus, Macherey-Nagel). Total carbohydrate content was determined using a calibration curve of different concentrations of a glucose standard solution.

Lipids were extracted using a modified Bligh and Dyer method as described previously (Pereira et al., 2011). Briefly, freeze-dried biomass was dispersed using an Ultra-Turrax T10B disperser (IKA-Werke, Germany) in a mixture of chloroform, methanol and water (2:1:1). After phase separation by centrifugation, the chloroform phase containing the lipids was transferred to a new tube. A known volume of chloroform was pipetted to a pre-weighed glass vial and evaporated overnight. The weight of the dried residues was divided by the initial DW to determine the lipid fraction.

2.4.6. Fatty acids

The profile of fatty acid methyl esters (FAMEs) of samples from the inoculum and harvested after three days were analyzed following a protocol described in Pereira et al. (2012) with slight modifications. Freeze-dried biomass was dispersed for 1.5 min in a solution of methanol and acetyl chloride (20:1, v/v) containing an internal standard (Tricosanoic acid C23:0, Sigma-Aldrich, Portugal). After the addition of *n*-hexane, the fatty acids were derivatized for 60 min at 70 °C. FAMEs were then sequentially extracted two times from the reaction mixture using *n*-hexane. Hexane extracts were dried with anhydrous sodium sulphate, filtered and evaporated under a gentle nitrogen flow. The dried extracts were resuspended in hexane and stored at − 20 °C until GC–MS analysis. FAME profiles were analyzed by a Scion 456/GC Scion TQ MS (Bruker, USA) equipped with a 30-m ZB-5MS capillary column (30 × 0.25 mm of internal diameter with 0.25 μm film thickness; Phenomenex) using helium as a carrier gas. Elution was carried at 1 mL min^{-1} using an injection temperature of 300 °C in split-less mode with the following temperature settings: 60 °C for 1 min, 30 °C min^{-1} to 120 °C, 4 °C min^{-1} to 250 °C and 20 °C min^{-1} to 300 °C, hold for 4 min. For identification and quantification of FAMEs, calibration curves using Supelco® 37 Component FAME Mix (Sigma-Aldrich, Portugal) were established.

2.5. Statistical analysis

Data were tested for normality using the Shapiro-Wilk test (XLStat software, Vers. 2016.02.27444, Addinsoft, USA). ANOVA and Tukey's HSD post hoc test were performed for the comparison of means of treatments with a confidence interval of 95% if not otherwise indicated.

3. Results and discussion

3.1. Mutant isolation

To obtain carotenoid-rich mutants of *T. striata*, random mutagenesis using the alkylating agent EMS with subsequent selection of mutants resistant to the herbicide norflurazon was performed. Mutant selection on the herbicide norflurazon was used to enhance the selective pressure to find cells mutated in genes involved in the carotenoid biosynthetic pathway, in particular the phytoene desaturase (*PDS*) gene (Breitenbach et al., 2001). Afterwards, a killing curve to the mutagenic agent EMS was established to find a concentration leading to a 5–10% survival, which usually decreases the occurrence of multiple secondary mutations that lead to detrimental growth. The WT strain killing curve displayed the expected sigmoidal course and a survival rate of 8.68% was obtained by using an EMS concentration of 250 mM (Fig. 1A). The subsequent selection on norflurazon led to the isolation of 20 herbicide-resistant colonies, of which one colony, here named ED5, revealed a 24% carotenoid content increase as compared with the WT. Therefore, this mutant strain was subjected to further selection by fluorescence activated cell sorting (FACS; Pereira et al., 2018). As cultures were not axenic, a first gate (Chl) was set to select only for chlorophyll positive cells using the red fluorescence (695 nm) emitted by chlorophyll *a* (FL1, Fig. 1B and 1C). This first gated subpopulation was then sorted for cells with higher carotenoid fluorescence (Car) at the emission wavelength of 530 nm (FL2, Fig. 1D and 1E). The emission in the green range of the electromagnetic spectrum has been related with carotenoid contents previously (Chen et al., 2017; Kleinegris et al., 2010; Schüler et al., 2020b). The ED5 strain displayed six times more cells in this gate as compared with the WT, representing 12.9 and 2.08% of total carotenoid positive cells, respectively (Fig. 1D and 1E). After cell sorting of the carotenoid gate of ED5, 48 colonies were able to grow on 96-well plates. Eight mutant strains were selected for analysis of carotenoid profiles by HPLC upon testing their resistance to norflurazon and growth performance. The mutants B11 and G8 showed significant higher carotenoid contents as compared with the WT, 4.8 and 4.0 mg g^{-1} DW, respectively (Fig. 1F). However, only B11 showed a significantly different carotenoid content compared to ED5. Furthermore, both mutants have been maintained in the lab over one year without changes in their norflurazon-resistant and increased carotenoid contents. Therefore, ED5 and B11 were selected for the following growth experiment and gene expression analysis.

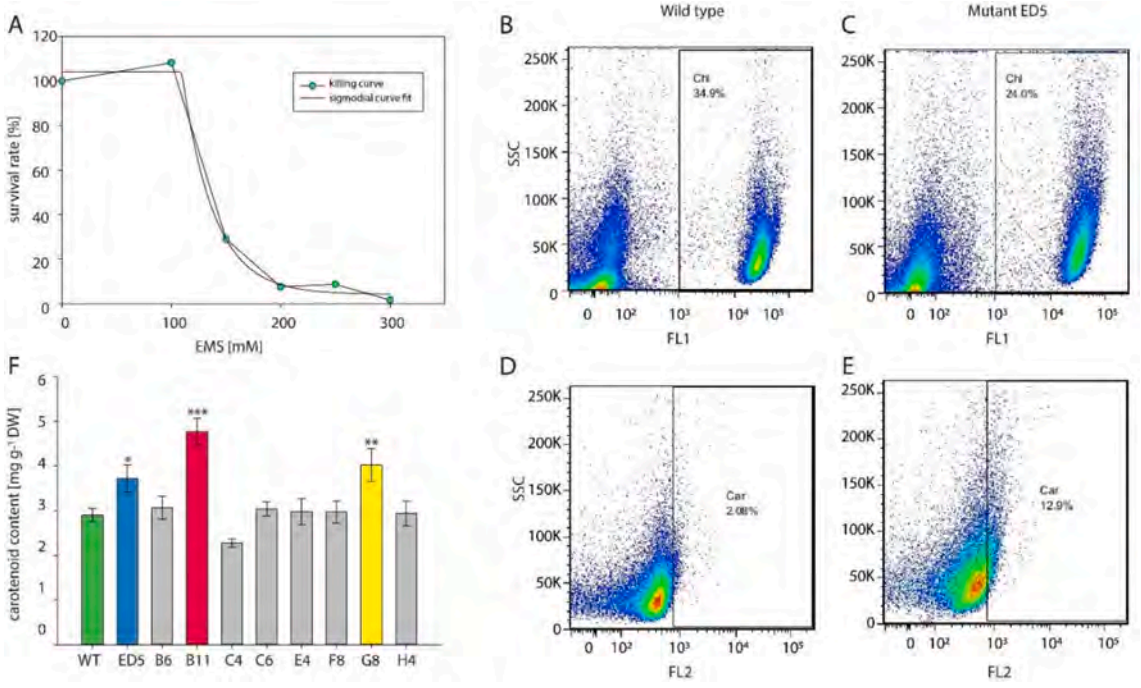

Fig. 1. Isolation of carotenoid-rich mutants of *T. striata*. A killing curve of the WT using different concentrations of EMS was established (A). Fluorescence activated cell sorting (FACS) of WT and ED5 strains showing the gates for chlorophyll (Chl) positive cells (B, C) and the gates for sorting of carotenoid (Car) positive cells (D, E). Carotenoid contents of the WT, ED5 and other mutants isolated by FACS determined by HPLC ($n = 3$, mean ± SD). Significant differences (Dunnetts test) to the WT are represented by one ($p < 0.05$), two ($p < 0.01$) or three ($p < 0.001$) asterisks (F).

3.2. Growth performance and pigment contents of WT and mutants under different growth conditions

The growth performance and pigment contents of the WT and two of the most promising mutants, ED5 and B11, was followed under mesophilic (20 °C, 100 μmol m^{-2} s^{-1}) and stress conditions (30 °C, 380 μmol m^{-2} s^{-1}). The growth curves of all three strains showed the beginning of exponential phase with a lag phase in the first two days. Upon three days of growth, no significant differences between the WT and mutant microalgae could be observed under all growth conditions. However, the WT culture reached a slightly higher biomass concentration under stress conditions than ED5 and B11 cultures: 0.74 ± 0.07, 0.53 ± 0.07 and 0.58 ± 0.08 g L^{-1}, respectively (data not shown). Remarkably, the chlorophyll contents of the WT were significantly higher than those of the mutants under both conditions tested (Fig. 2). At mesophilic conditions, after three days of growth, chlorophyll reached the highest content in the WT followed by ED5 and B11: 40.5 ± 2.6, 33.8 ± 1.1 and 25.5 ± 2.1 mg g^{-1} DW, respectively. Chlorophyll contents of 35 mg g^{-1} DW have been previously reported in this species (Pereira et al., 2019). Conversely, stress (heat stress and higher light) conditions led to lower chlorophyll contents in all three strains, 18.7 ± 1.6, 7.96 ± 0.95 and 13.9 ± 0.4 mg g^{-1} DW, respectively. A higher chlorophyll content under lower (mesophilic) light conditions is a common phenomenon which can be explained by the need for better light utilization and, therefore, the increase in chlorophyll molecules (da Silva Ferreira and Sant'Anna, 2017). When comparing carotenoid contents, the WT showed significantly higher contents than both ED5 and B11 mutant strains at the beginning of the experiment: 6.69 ± 0.12, 5.04 ± 0.41 and 4.63 ± 0.13 mg g^{-1} DW, respectively. However, upon three days of growth, carotenoid contents in both mutants increased significantly, overtaking the

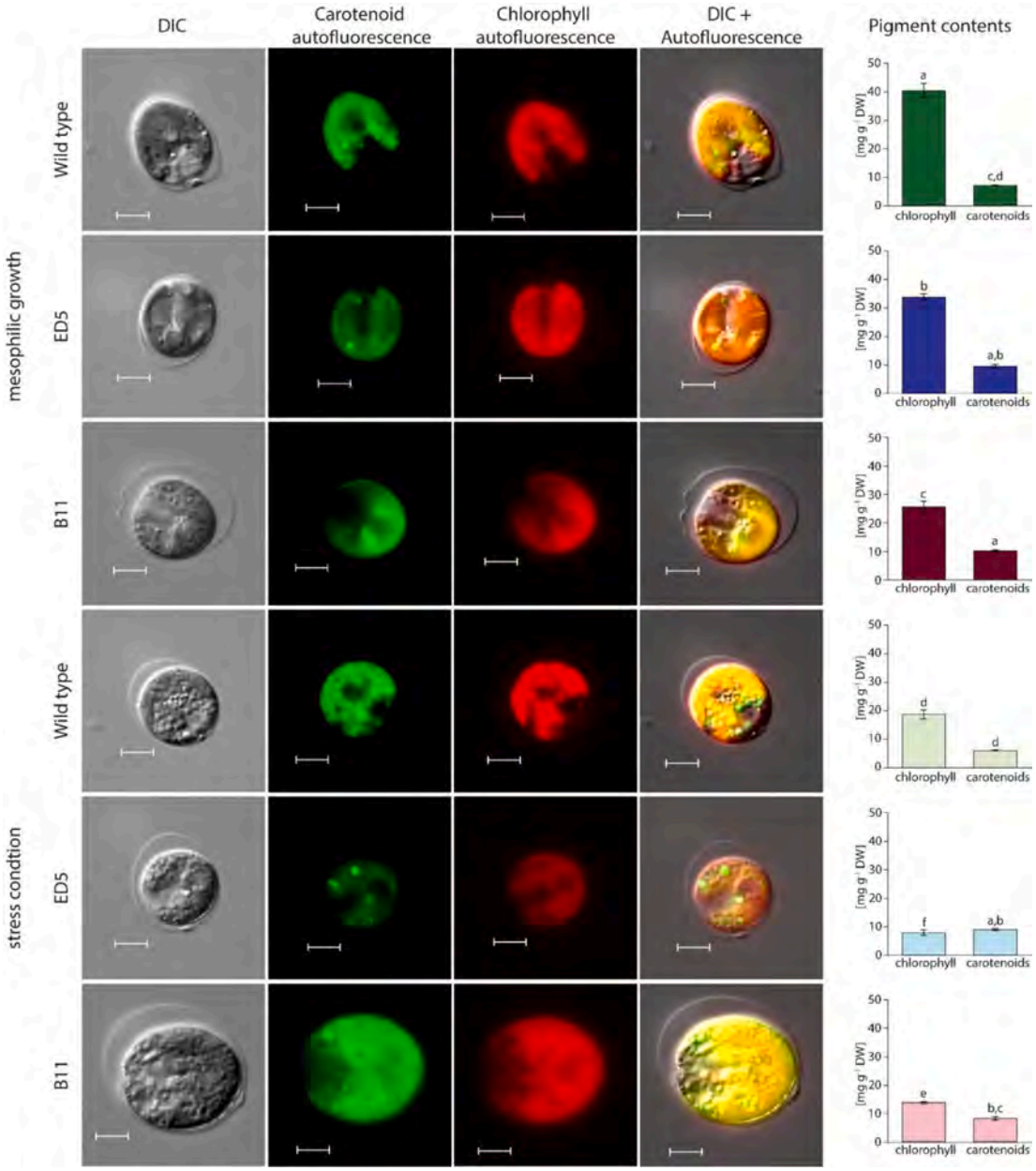

Fig. 2. Microscopic observations and pigment contents of *T. striata* WT, ED5 and B11 strains under mesophilic (20 °C, 100 μmol m^{-2} s^{-1}) and stress (30 °C, 380 μmol m^{-2} s^{-1}) conditions. Chlorophyll and carotenoid contents were analyzed of the cultures grown for three days (n = 3, mean ± SD). Different letters over the bars indicate significant differences between samples of the same pigment ($p < 0.05$). Images were taken using differential interference contrast (DIC) and the autofluorescence of carotenoid and chlorophyll pigments (38 HE and 50 filter sets, respectively). Scale bar = 5 μm.

WT by up to 47%. The highest carotenoid contents (10.2 ± 0.4, 9.48 ± 0.67 and 7.17 ± 0.20 mg g^{-1} DW) could be found under mesophilic growth conditions, while stress conditions led to slightly lower carotenoid contents: 8.36 ± 0.59, 9.01 ± 0.41 and 6.12 ± 0.14 mg g^{-1} DW for B11, ED5 and WT, respectively (Fig. 2). Microscopic observations revealed that WT and mutant cells under mesophilic growth conditions displayed similar cell sizes (≈15 μm). When comparing chlorophyll autofluorescence, the WT showed a chloroplast with its typical U-shape in these cells; however, the plastid autofluorescence in the mutant cells seemed to be more diffuse. Furthermore, the autofluorescence in B11 microalgae appeared less intense than those of the other two strains, which is in agreement with the lower chlorophyll contents under mesophilic growth conditions. The carotenoid (38 HE) fluorescence in all three strains has the same shape as the chlorophyll (50 HE) fluorescence, confirming the assumption of a previous study on this species that the carotenoids seem to accumulate in the chloroplast (Schüler et al., 2020b). However, the carotenoid to chlorophyll fluorescence ratio in both mutants is more intense than that of the WT, which becomes evident in the DIC + autofluorescence overlay; in this case, mutant cells display a more intense yellowish hue due to higher carotenoid fluorescence and lower chlorophyll fluorescence. Interestingly, under stress conditions, B11 microalgae are on average 50% larger as compared with WT and ED5 cells. The chlorophyll autofluorescence appears less intense in both mutants than WT under these conditions. Conversely, carotenoid autofluorescence is more intense in B11 microalgae, while ED5 cells show several intense spots of fluorescence against a less intense fluorescent background. These observations confirm the differences measured in pigment contents. Indeed, a larger cell and/or spots emitting intense carotenoid autofluorescence could be the reason for increased carotenoid contents in the mutants.

3.3. Carotenoid profile of WT and mutant strains under different growth conditions

The carotenoid profile of the WT under mesophilic growth conditions did not change significantly during the experiment, showing mainly *β*–carotene (3.65 ± 0.20 mg g^{-1} DW) and lower amounts of violaxanthin (1.14 ± 0.06 mg g^{-1} DW), neoxanthin (1.08 ± 0.07 mg g^{-1} DW) and lutein (1.31 ± 0.10 mg g^{-1} DW) after three days of growth (Fig. 3). Only zeaxanthin contents increased, reaching their highest level (0.05 ± 0.003 mg g^{-1} DW) after three days of growth. However, under stress conditions, zeaxanthin and lutein contents increased significantly to respectively 0.07 ± 0.003 and 2.65 ± 0.13 mg g^{-1} DW after three days, being accompanied by decreased *β*–carotene (1.48 ± 0.10 mg g^{-1} DW) and neoxanthin (0.74 ± 0.04 mg g^{-1} DW) contents. These observations are in agreement with a previous study on this strain (Schüler et al., 2020b); lower light intensities at mesophilic growth conditions (100 μmol m^{-2} s^{-1}) led to an increase in light harvesting pigments, while photoprotective pigment levels rose under heat and high light stress. Moreover, the violaxanthin cycle is an important photoprotective mechanism for cells to adapt to changing environmental conditions; under lower light, violaxanthin is usually increased while WT cells show enhanced zeaxanthin levels under high light (Jahns et al., 2009). The pigment profile of ED5 cells was similar to that of the WT under mesophilic growth conditions, though with significantly higher contents of *β*-carotene (4.87 ± 0.44 mg g^{-1} DW) and violaxanthin (1.43 ± 0.07 mg g^{-1} DW), but equivalent neoxanthin contents (1.15 ± 0.03 mg g^{-1} DW) at day 3 (Fig. 3). Moreover, up to 1.6-fold higher lutein and 2.1-fold

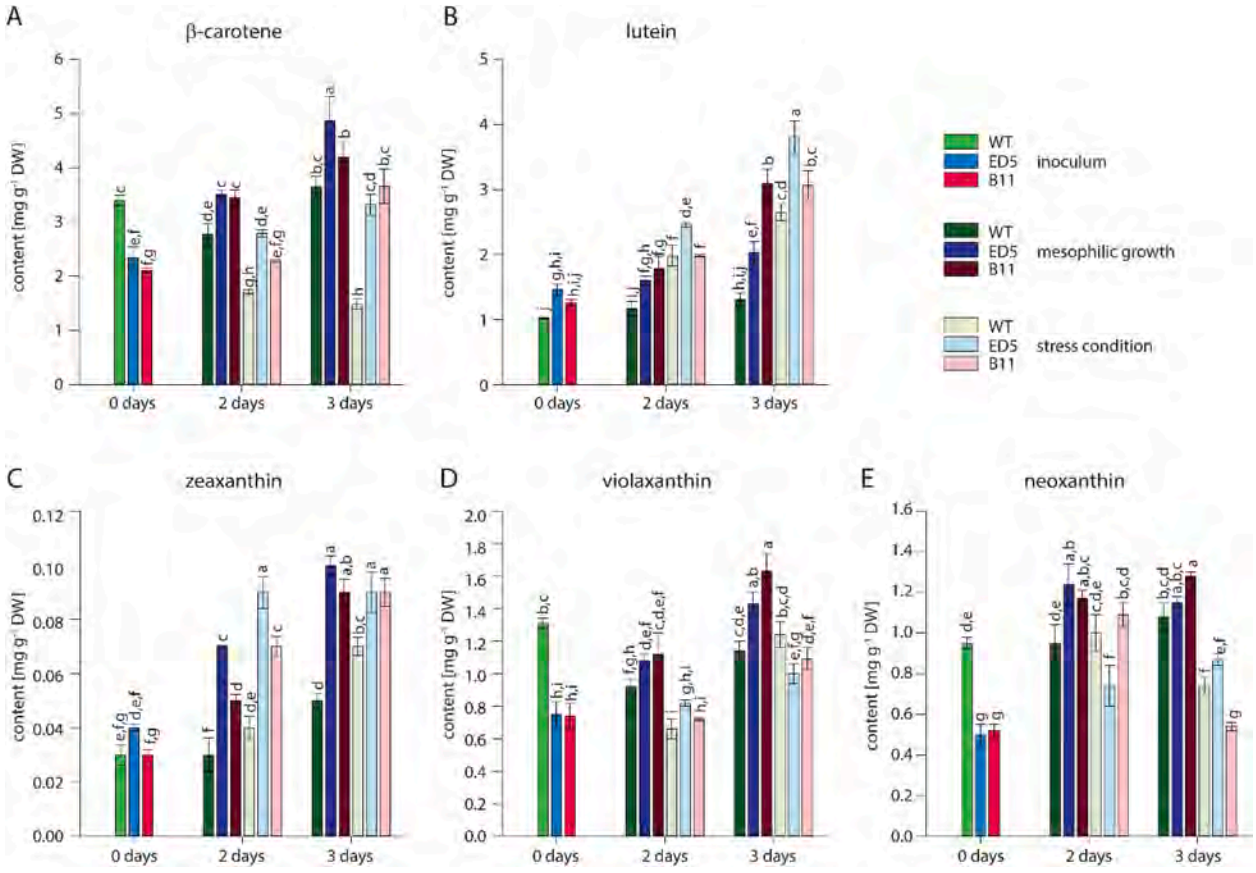

Fig. 3. Carotenoid contents of *T. striata* WT, ED5 and B11 strains under mesophilic (20 °C, 100 μmol m^{-2} s^{-1}) and stress (30 °C, 380 μmol m^{-2} s^{-1}) conditions. Contents of *β*-carotene (A), lutein (B), zeaxanthin (C), violaxanthin (D) and neoxanthin (E) were quantified using RP-HPLC in the biomass harvested from the inoculum and after two and three days (n = 3, mean ± SD). Different letters over the bars indicate significant differences between samples for each compound (p < 0.05).

higher zeaxanthin contents than those in WT cells were observed under mesophilic growth conditions, reaching their highest values after three days (2.03 ± 0.17 mg g^{-1} DW and 0.10 ± 0.004 mg g^{-1} DW, respectively). Under stress conditions, zeaxanthin content remained relatively high (0.09 ± 0.01 mg g^{-1} DW). However, lutein content rose to 3.81 ± 0.25 mg g^{-1} DW on the third day of growth, which corresponded to a 1.4-fold increase compared to WT levels (Fig. 3B). Moreover, ED5 microalgae showed a 2.3-fold increase in β-carotene content (3.32 ± 0.19 mg g^{-1} DW) when compared to that in WT cells under stress conditions (Fig. 3A). Taken together, these observations suggest that in this mutant both branches of the carotenoid pathway are more active than in the WT, regardless of the growth conditions. The B11 mutant strain is a derivate of ED5 cells and was isolated under low light conditions (45 μmol m^{-2} s^{-1}). Remarkably, after three days of growth under mesophilic conditions, B11 microalgae displayed not only the expected high β-carotene (4.20 ± 0.27 mg g^{-1} DW), violaxanthin (1.63 ± 0.11 mg g^{-1} DW) and neoxanthin (1.28 ± 0.02 mg g^{-1} DW) contents but also relatively high zeaxanthin levels (0.09 ± 0.005 mg g^{-1} DW). Moreover, the lutein contents showed a 2.4-fold increase as compared to the WT, i.e., 3.09 ± 0.23 mg g^{-1} DW (Fig. 3B). Such increase in photoprotective pigments by B11 microalgae may be linked to a higher light sensibility and the exposure to 100 μmol m^{-2} s^{-1} under mesophilic growth was perceived by the cells as high light. Moreover, this mutant displayed the lowest chlorophyll contents as compared with those of other strains under mesophilic growth (Fig. 2), which might also be related to the stress sensed under this condition. Under stress conditions, lutein (3.07 ± 0.22 mg g^{-1} DW) and zeaxanthin (0.09 ± 0.005 mg g^{-1} DW) contents did not change significantly as compared with those found under mesophilic growth conditions (Fig. 3). However, β-carotene, violaxanthin and neoxanthin contents decreased to 3.66 ± 0.32, 1.09 ± 0.07 and 0.54 ± 0.02 mg g^{-1} DW, respectively. Nevertheless, β-carotene content in B11 cells was the highest observed under stress conditions after three days, representing a 2.5-fold increase as compared with WT levels.

3.4. Transcript expression analysis of carotenogenic genes in WT and mutants

For a better understanding of the above-mentioned carotenoid contents in WT and mutant strains ED5 and B11, the gene expression analysis of the carotenoid biosynthetic genes, namely *PSY*, *PDS*, *LCYB*, *LCYE*, *CHYB* and *CYP97C3*, was performed at the beginning and after one day of growth under either mesophilic or stress conditions (Fig. 4). Phytoene synthase (PSY) catalyzes the first step of the carotenoid pathway leading to phytoene (Fig. 5), which is often considered to be a rate-limiting step of the pathway (Cordero et al., 2011). The transcript levels of this enzyme did not change significantly in the WT cells throughout the experiment. Conversely, in both mutants ED5 and B11 under stress conditions, the *PSY* transcript levels were significantly upregulated, 1.9- and 1.5-fold, respectively, compared to the levels of WT cells (Fig. 4A). Down in the pathway, phytoene is then converted to ζ-carotene by phytoene desaturase (PDS), which has been identified as a rate-limiting enzyme in lutein biosynthesis (Li et al., 2013).

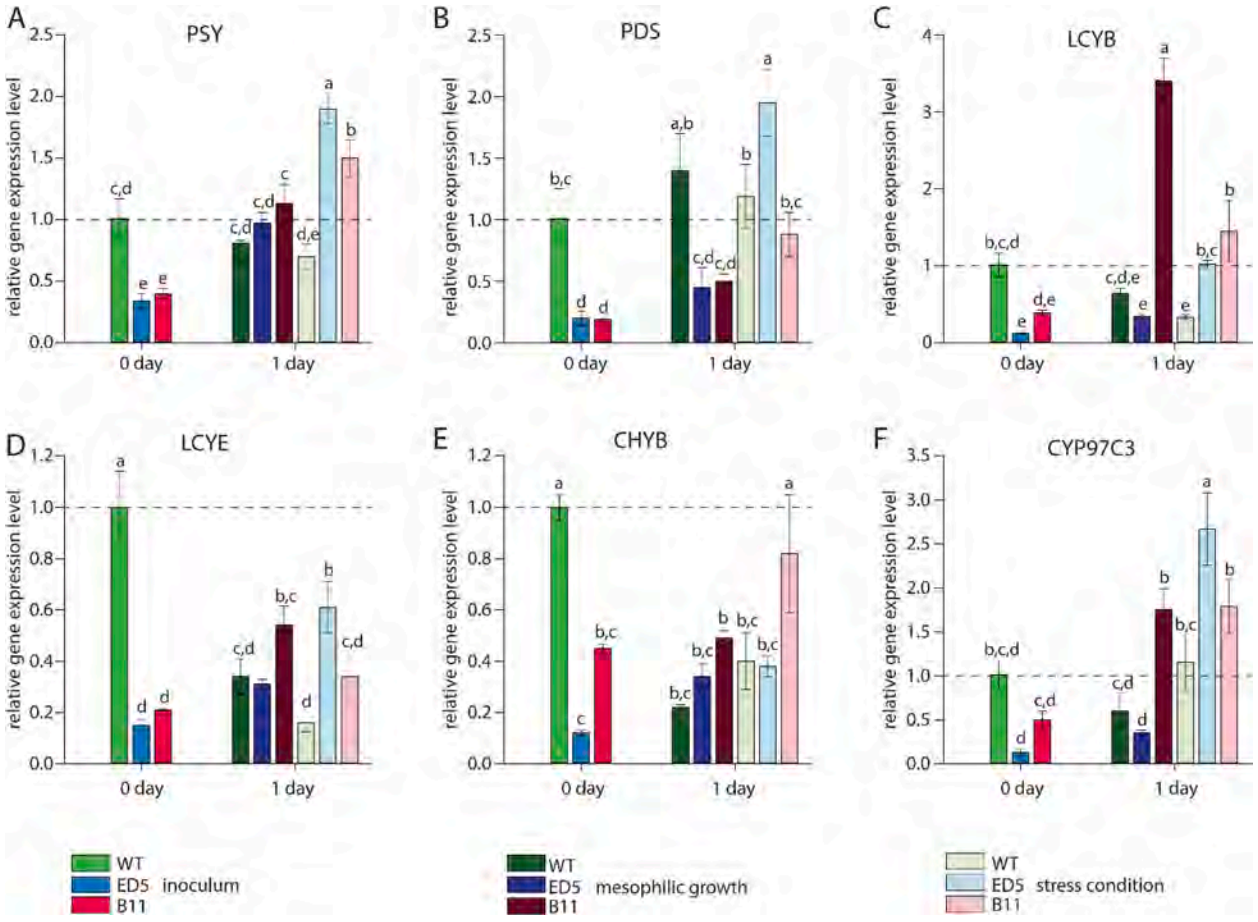

Fig. 4. Relative transcript steady-state levels of genes involved in carotenoid biosynthesis in *T. striata* WT, ED5 and B11 cells under mesophilic (20 °C, 100 μmol m^{-2} s^{-1}) and stress (30 °C, 380 μmol m^{-2} s^{-1}) conditions. RNA was extracted from the inoculum and after one day of growth ($n = 3$). Relative gene expression levels of phytoene synthase (PSY) (A), phytoene desaturase (PDS) (B), lycopene-β-cyclase (LCYB) (C), lycopene-ε-cyclase (LCYE) (D), β-carotene hydroxylase (CHYB) and cytochrome P450 ε-ring hydroxylase (CYP97C3) (E) were analyzed by the $2^{-\Delta\Delta Ct}$ method based on cycle threshold (Ct) values using 18S ribosomal RNA as an internal control (mean ± SD). Different letters over the bars indicate significant differences between samples of the same gene ($p < 0.05$).

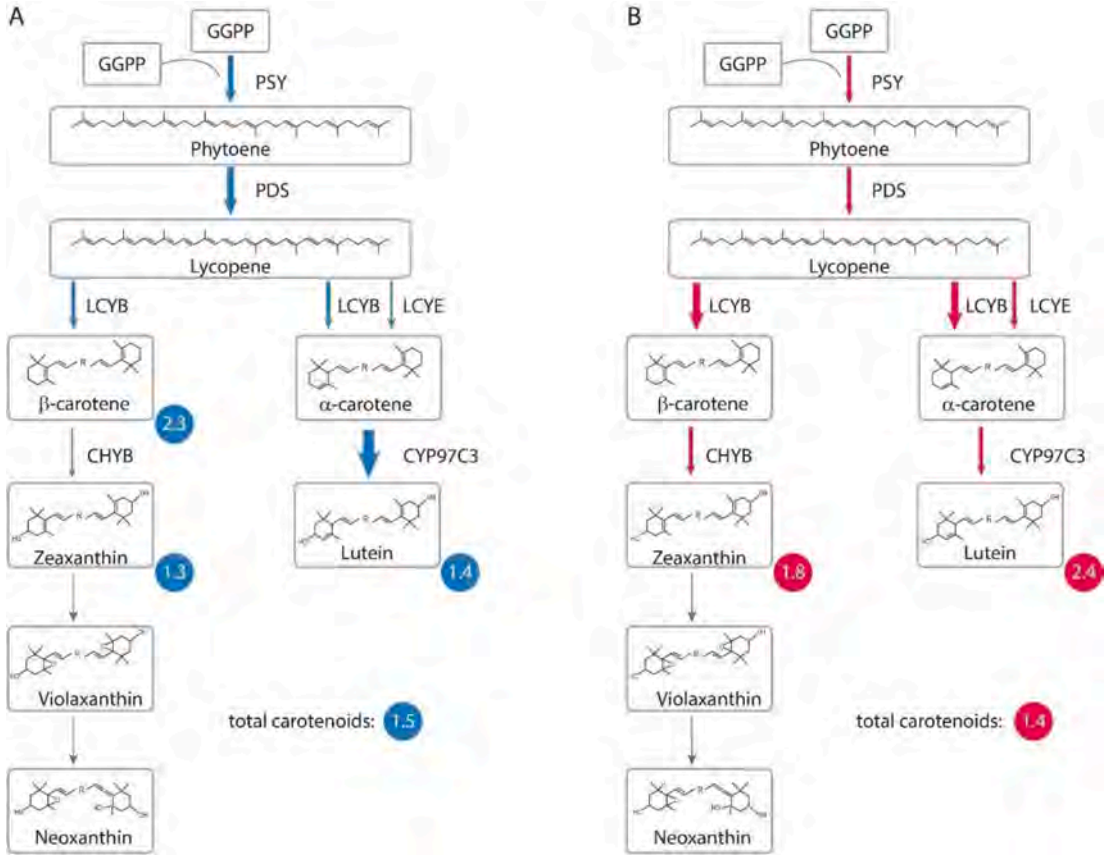

Fig. 5. Simplified carotenoid biosynthetic pathway in *T. striata* ED5 (A, blue) and B11 (B, red) strains. The numbers to the right of each metabolite correlate with the fold increase in carotenoid levels as compared to the WT. The thickness of the arrows indicates the relative gene expression of transcripts coding for the corresponding enzyme as compared to the WT. The fold increases shown for ED5 and B11 are those of cells under stress (30 °C, 380 μmol m^{-2} s^{-1}) and mesophilic (20 °C, 100 μmol m^{-2} s^{-1}) conditions, respectively. PSY, phytoene synthase; PDS, phytoene desaturase, LCYB, lycopene-*β*-cyclase; LCYE, lycopene-*ε*-cyclase, CHYB, *β*-carotene hydroxylase; and CYP97C3, heme-containing cytochrome P450 *ε*-ring hydroxylase. (For interpretation of the references to colour in this figure legend, the reader is referred to the web version of this article.)

Interestingly, *PDS* transcript levels were increased 2.0-fold in ED5 cells under stress conditions as compared with the WT (Fig. 4B), matching the higher lutein contents observed in ED5 cells (Fig. 3B). For the WT and B11 and under mesophilic growth conditions, no significant changes in the levels of transcripts coding for this enzyme were observed throughout the experiment. Nevertheless, when comparing transcript levels between B11 cells, *PDS* underwent a 3.7-fold upregulation under stress conditions as compared with the beginning of the experiment (Fig. 4B). The higher expression of *PSY* and *PDS* genes in the mutant cells under high light (stress conditions, 30 °C, 380 μmol m^{-2} s^{-1}) is in accordance with previous studies on *Haematococcus pluvialis*, *Dunaliella salina*, *Chlamydomonas* spp. and *Chlorella* (*Chromochloris*) *zofingiensis* (Coesel et al., 2008; Cordero et al., 2012; Couso et al., 2012; Ma et al., 2019; Steinbrenner and Linden, 2003). After the synthesis of lycopene, the carotenoid pathway splits into two branches (Fig. 5). In one branch, lycopene-*β*-cyclase (LCYB) catalyzes the formation of *β*-carotene, which is further converted by *β*-carotene hydroxylase (CHYB) to zeaxanthin, followed by the biosynthesis of violaxanthin and neoxanthin. In the other branch, the activity of both lycopene-*β*- and *ε*-cyclases (LCYE) lead to the biosynthesis of *α*-carotene, which is hydroxylated to lutein by the stepwise reaction of two heme-containing cytochrome P450 monooxygenases, namely *β*-ring hydroxylase CYP97A5 and *ε*-ring hydroxylase CYP97C3. In ED5 and B11 cells, the *CYP97C3* transcript levels were upregulated under stress conditions, rising 2.7- and 1.8-fold when compared to the levels found in WT cells (Fig. 4F). Together with the higher expression of the upstream genes involved in the carotenoid biosynthetic pathway, this observation agrees with the higher lutein contents observed in these strains as compared with the WT (Fig. 3B). Moreover, high light intensity has previously been shown to increase the expression of *CYP97C3* in *Chlamydomonas* sp. (Cordero et al., 2012). As has already been assumed from the carotenoid profile of B11 microalgae under mesophilic growth conditions, the light intensity of 100 μmol m^{-2} s^{-1} seemed to be sensed as high light by these mutant cells. The 1.7-fold upregulation of *CYP97C3* transcript levels, when compared with those of the WT, provides another evidence for this assumption (Fig. 4F). Remarkably, these conditions led to the highest *LCYB* gene expression in B11 cells, resulting in a 3.4-fold increase compared to the levels found in WT cells. Low temperature (20 °C), as compared with high temperature (35 °C), has previously been reported to increase the *LCYB* gene expression in *Chlamydomonas* sp. (Ma et al., 2020). Therefore, temperature rather than light intensity might have been the most important factor for the observed higher expression levels of *LCYB* under mesophilic growth than under stress, representing only a 1.4-fold increase in B11 cells as compared with the WT levels. When comparing transcript levels between the beginning and after one day of the experiment, the expression levels of all investigated genes were upregulated in both mutants under both mesophilic and stress conditions. This observation matches the observed ≈2-fold increase in carotenoid contents in these strains after three days of growth as compared with the beginning of the experiment. However, carotenoid contents did not increase with cultivation time in WT cells, which can be explained by the absence of any observable increase in the expression of the corresponding genes (Fig. 4). The observed changes in carotenoid contents might be due to shifts from one metabolite to the other, most probably controlled post-

transcriptionally by changing the activities of the corresponding enzymes under different environmental conditions.

To sum up, the 1.5-fold increased carotenoid content ($n = 3$) of ED5 microalgae under stress conditions as compared with the WT can be correlated with the higher *PSY* and *PDS* gene expression of respectively 1.9- and 2.0-fold, affecting the initial enzymes of the pathway (Fig. 5). Moreover, the higher lutein contents observed in this mutant are probably a result of a higher expression of the *CYP97C3* gene. Conversely, in B11 microalgae, the observed 1.4-fold increase in carotenoid contents as compared with the WT took place under both growth conditions tested. However, under mesophilic growth conditions, higher *LCYB* and *CYP97C3* transcript levels seemed to have been the most decisive factors for the 2.4-fold increase in lutein found in B11 cells when compared with WT microalgae (Fig. 5). Conversely, under stress conditions, high *PSY* and *PDS* gene expression apparently led to the observed 2.5-fold increase in β-carotene contents. Interestingly, the *CYP97C3* transcript levels remained high under these conditions, agreeing with the high lutein levels found in this strain, regardless of the growth conditions. Interestingly, in the norflurazon-resistant mutants, not only the *PDS* transcript levels were affected but also those of other carotenogenic genes. These observations provide further evidence that this pathway possesses multiple regulatory mechanisms, which are difficult to target in a metabolic engineering approach.

3.5. Biochemical composition and fatty acid profile of WT and mutants under different growth conditions

To elucidate possible changes and better understand the potential of the novel strains ED5 and B11 in future products, the protein, carbohydrate and lipid contents and fatty acid profiles were compared to those of the WT under mesophilic growth and stress conditions.

The protein contents of the inoculum did not show any significant differences between the three strains. Under mesophilic growth, maximum protein content was reached in all three strains, which was on average 24.7 ± 1.7% of DW (Table 1). Protein contents in this range have been reported previously in microalgae of the genus *Tetraselmis* under these growth conditions (Kim et al., 2016). However, under stress conditions, protein contents decreased in all three strains, particularly in B11 cells (13.3 ± 0.6% DW). Reduced protein contents under heat stress have been reported earlier in other marine microalgae and can be related to a breakdown of housekeeping proteins in order to have enough amino acids for a more reduced proteome geared to protect the cell against heat-induced denaturation (Renaud et al., 2002).

The carbohydrate content of the WT in the inoculum was 43.1 ± 2.2% of DW and remained constant when cells were grown under stress (Table 1). However, under mesophilic growth the carbohydrate content decreased to 28.4 ± 2.8% of DW. Carbohydrate contents in this range have been reported in *Tetraselmis striata* CTP4 previously (Schulze et al., 2017). The mutant ED5 showed carbohydrate contents similar to those of the WT, achieving the highest content of 48.5 ± 4.2% of DW under stress conditions. Remarkably, B11 cells contained the lowest carbohydrate content in the beginning of the experiment, which increased during the growth under both conditions test overtaking those of the WT. Highest carbohydrate contents of 61.6 ± 3.8% of DW were recorded in the B11 strain under stress conditions (30 °C, 380 μmol m^{-2} s^{-1}). Increased temperature and light intensities have previously been reported to increase carbohydrate contents in species belonging to the genus *Tetraselmis* (Michels et al., 2014; Shin et al., 2016).

Table 1
Protein, lipid and carbohydrate contents in WT, ED5 and B11 strains under mesophilic (20 °C, 100 μmol m^{-2} s^{-1}) and stress (30 °C, 380 μmol m^{-2} s^{-1}) conditions after three days of growth ($n = 3$, mean ± SD). Significant differences between samples of the same compound are indicated by different letters ($p < 0.05$).

conditions	strain	proteins (% DW)	lipids (% DW)	carbohydrates (% DW)
inoculum	WT	23.7 ± 0.3^{a}	8.26 ± 0.08^{b}	$43.1 \pm 2.2^{b,c}$
	ED5	24.8 ± 1.2^{a}	7.90 ± 0.11^{b}	n.d.
	B11	$21.8 \pm 0.3^{a,b}$	7.31 ± 0.28^{b}	25.3 ± 1.1^{e}
mesophilic	WT	25.7 ± 5.1^{a}	8.64 ± 0.27^{b}	$28.4 \pm 2.8^{d,e}$
	ED5	25.7 ± 3.6^{a}	9.19 ± 1.01^{b}	$30.7 \pm 1.9^{c,d,e}$
	B11	$22.7 \pm 0.5^{a,b}$	9.78 ± 0.12^{b}	45.6 ± 6.7^{b}
stress	WT	$17.5 \pm 3.6^{a,b}$	17.1 ± 0.3^{a}	$40.0 \pm 7.2^{b,c,d}$
	ED5	$17.1 \pm 1.5^{a,b}$	9.26 ± 1.46^{b}	48.5 ± 4.2^{b}
	B11	13.3 ± 0.6^{b}	14.0 ± 2.7^{a}	61.6 ± 3.8^{a}

n.d. = not determined due to insufficient amount of biomass.

The lipid content of all the three strains at the beginning of the experiment and at mesophilic growth conditions was between 8 and 10% of DW (Table 1). This is in agreement with previous reports on this species, presenting lipid contents of about 10% of DW under mesophilic growth conditions (Pereira et al., 2016; Schulze et al., 2017). Under stress conditions, the lipid content of WT and B11 increased significantly to 17.1 ± 0.3 and 14.0 ± 2.7% of DW, respectively. This increase is most probably related to the heat stress and higher light intensity, conditions known to increase lipid contents in marine microalgae (Nogueira et al., 2015). Under unfavorable conditions, lipids in the form of triacylglycerols serve as storage compounds for carbon and energy. Conversely, lipid contents in the mutant ED5 did not change significantly under stress conditions. One explanation could be that instead of being used for lipid biosynthesis, carbon is being diverted to carbohydrate and carotenoid production.

The fatty acid profile of WT, ED5 and B11 strains contained palmitic (C16:0), hexadecatetraenoic (C16:4), oleic (18:1) and linoleic (LA, C18:2*n-6*) acids, which corresponded to 70% of TFA. The remaining 20 to 30% of TFA were composed of palmitoleic (C16:1), hexadecatrienoic (C16:3*n-3*), stearidonic (SDA, C18:4*n-3*) and eicosapentaenoic (EPA, C20:5*n-3*) acids (Table 2). These fatty acid profiles are comparable to those of previous studies on this strain (Pereira et al., 2019; Schulze et al., 2017). Remarkably, under all tested conditions, the fatty acid profile in ED5 microalgae showed an enrichment of the *n*-3 fatty acids SDA and EPA as compared to the WT (Table 1). The highest content of EPA achieved was 4.41 ± 0.07 mg g^{-1} DW and could be found in the cells of ED5 microalgae in the beginning of the experiment. The EPA content also increased in B11 microalgae as compared with the WT, corresponding to 2.88 ± 0.29 mg g^{-1} DW under stress conditions. Furthermore, the precursor LA of these *n*-3 fatty acids was significantly decreased in both mutants as compared with the WT at the beginning of the experiment and remained at a lower level throughout the experiment. These observations may be explained by the resistance of the strains to the herbicide norflurazon and, therefore, a possible higher activity of Δ6 desaturases. However, further studies of the expression profiles of the fatty acid biosynthesis enzymes are needed to confirm this assumption.

Because changes were observed in different metabolites classes, it seems as though the mutations generated have a pleiotropic effect on the overall metabolism of the microalgal cell. These results highlight the fact that mutations might affect the expression of several genes in diverse metabolic pathways. These changes can be brought about by a mutation in a gene coding for a regulatory factor (e.g., transcription factor) or a single biosynthetic enzyme. Although the first possibility has an immediate pleiotropic potential, the second scenario might affect the metabolism via multiple metabolite feedback loops, also resulting in changes in the expression of multiple genes. In any case, these results underline the complexity of biological systems and the inherent difficulty of targeting a specific gene to obtain the desired phenotype.

Moreover, the protein, carbohydrate and lipid contents of WT and mutant strains under mesophilic conditions are similar to those reported in a recent study of this strain produced industrially and could therefore find their application in food or feed products (Pereira et al., 2019). Additionally, the presence of antioxidant compounds such as carotenoids and EPA could provide further health-promoting effects on both animals and humans (Nethravathy et al., 2019). However, the

Table 2
Fatty acid profiles of *T. striata* WT, ED5 and B11 strains after three days of growth under mesophilic (20 °C, 100 μmol m^{-2} s^{-1}) and stress (30 °C, 380 μmol m^{-2} s^{-1}) conditions ($n = 3$, mean ± SD). Linoleic (LA), stearidonic (SDA) and eicosapentaenoic (EPA) acid are shown in percentage of total fatty acids (TFA) and in mg g^{-1} DW. Significant differences between samples of the same compounds are indicated by different letters ($p < 0.05$).

conditions	strain	LA C18:2 (% TFA)	LA C18:2 (mg g^{-1} DW)	SDA C18:4 (% TFA)	SDA C18:4 (mg g^{-1} DW)	EPA C20:5 (% TFA)	EPA C20:5 (mg g^{-1} DW)
inoculum	WT	17.2 ± 0.6^{a}	12.2 ± 0.4^{a}	5.59 ± 0.32^{d}	3.97 ± 0.05^{c}	2.79 ± 0.51^{d}	$1.99 \pm 0.5^{c,d}$
	ED5	5.38 ± 1.04^{c}	2.76 ± 0.73^{c}	14.8 ± 0.7^{b}	7.55 ± 0.17^{b}	8.67 ± 0.49^{a}	4.41 ± 0.07^{a}
	B11	7.46 ± 0.50^{c}	2.53 ± 0.14^{c}	12.2 ± 0.6^{c}	4.18 ± 0.70^{c}	$5.81 \pm 0.43^{b,c}$	$1.99 \pm 0.39^{c,d}$
mesophilic	WT	$9.27 \pm 0.88^{b,c}$	$5.10 \pm 0.15^{b,c}$	$14.5 \pm 0.4^{b,c}$	$8.01 \pm 0.98^{a,b}$	$3.83 \pm 0.21^{c,d}$	$2.12 \pm 0.30^{c,d}$
	ED5	7.63 ± 0.67^{c}	4.30 ± 0.91^{c}	17.8 ± 0.6^{a}	9.96 ± 1.13^{a}	$5.69 \pm 0.31^{b,c}$	3.20 ± 0.50^{b}
	B11	7.75 ± 2.12^{c}	4.00 ± 1.40^{c}	$14.4 \pm 0.4^{b,c}$	7.29 ± 0.65^{b}	$5.51 \pm 1.02^{b,c}$	$2.77 \pm 0.27^{b,c}$
stress	WT	12.3 ± 1.5^{b}	$6.26 \pm 1.49^{b,c}$	4.71 ± 1.24^{d}	2.41 ± 0.92^{c}	2.92 ± 0.49^{d}	1.47 ± 0.29^{d}
	ED5	$9.01 \pm 1.47^{b,c}$	4.44 ± 1.89^{c}	5.78 ± 0.90^{d}	2.70 ± 0.39^{c}	$6.67 \pm 1.01^{a,b}$	$3.12 \pm 0.44^{b,c}$
	B11	12.3 ± 1.1^{b}	$8.75 \pm 2.44^{a,b}$	4.27 ± 0.53^{d}	2.95 ± 0.32^{c}	$4.20 \pm 0.80^{c,d}$	$2.88 \pm 0.29^{b,c}$

consumption of the whole biomass by humans is hampered because this species has not yet been approved by the European Food Safety Agency (EFSA). Different applications to the pharmaceutical, nutraceutical, or cosmetic industry are thus conceivable upon setting up a biorefinery to yield the most value from a robust industrial microalga such as *T. striata* WT and its derivatives.

4. Conclusions

We successfully isolated two strains of the euryhaline microalga *Tetraselmis striata* CTP4 with improved carotenoid and EPA contents. The creation of non-GMO strains of biotechnologically relevant microalgae by random mutagenesis represents a powerful tool to gather knowledge of metabolic pathways and provides a cost-effective way of isolating improved strains with a promising future in the food, feed and pharmaceutical industries. Moreover, as *T. striata* has already been grown at large-scale, these non-GMO mutants can be considered as promising sources of carotenoids and EPA using processes that can be easily scaled up at industrial facilities.

Funding

This research was funded by FCT - Foundation for Science and Technology through project 055 ALGARED + 05 INTERREG V-A – España Portugal and UIDB/04326/2020 projects. LS and TS would like to acknowledge the FCT for awarding the doctoral research grants SFRH/BD/115325/2016 and SFRH/BD/140143/2018, respectively.

CRediT authorship contribution statement

Lisa M. Schüler: Conceptualization, Investigation, Data curation, Writing - original draft, Writing - review & editing, Validation. **Gabriel Bombo:** Conceptualization, Investigation, Writing - review & editing. **Paulo Duarte:** Investigation, Writing - review & editing. **Tamára F. Santos:** Conceptualization, Data curation, Investigation, Writing - review & editing, Validation. **Inês B. Maia:** Data curation, Investigation, Writing - review & editing. **Filipa Pinheiro:** Data curation, Investigation. **José Marques:** Data curation, Investigation. **Rita Jacinto:** Investigation, Writing - review & editing. **Peter S.C. Schulze:** Software, Writing - review & editing, Validation. **Hugo Pereira:** Conceptualization, Supervision, Writing - review & editing. **Luísa Barreira:** Supervision, Writing - review & editing, Validation, Funding acquisition. **João C.S. Varela:** Conceptualization, Supervision, Writing - review & editing, Validation, Funding acquisition.

Declaration of Competing Interest

The authors declare that they have no known competing financial interests or personal relationships that could have appeared to influence the work reported in this paper.

Acknowledgments

The authors acknowledge Maurícia Vinhas for all her work and support at the flow cytometry unit, CMBR, University of Algarve. The Microscopy Unit was partially supported by national Portuguese funding FCT: PPBI-POCI-01-0145-FEDER-022122. Furthermore, we would like to acknowledge Margarida Ribau Teixeira for the use of the HPLC system at the University of Algarve, financed by FCT grant UIDB/04085/2020 from CENSE, center for environmental and sustainability research.

Appendix A. Supplementary data

Supplementary data to this article can be found online at https://doi.org/10.1016/j.biortech.2021.125385.

References

Breitenbach, J., Zhu, C., Sandmann, G., 2001. Bleaching herbicide norflurazon inhibits phytoene desaturase by competition with the cofactors. J. Agric. Food Chem. 49 (11), 5270–5272. https://doi.org/10.1021/jf0106751.

Chen, J., Wei, D., Pohnert, G., 2017. Rapid estimation of astaxanthin and the carotenoid-to-chlorophyll ratio in the green microalga *Chromochloris zofingiensis* using flow cytometry. Mar. Drugs 15, 1–23. https://doi.org/10.3390/md15070231.

Coesel, S.N., Baumgartner, A.C., Teles, L.M., Ramos, A.A., Henriques, N.M., Cancela, L., Varela, J.C.S., 2008. Nutrient limitation is the main regulatory factor for carotenoid accumulation and for Psy and Pds steady state transcript levels in *Dunaliella salina* (Chlorophyta) exposed to high light and salt stress. Mar. Biotechnol. 10 (5), 602–611. https://doi.org/10.1007/s10126-008-9100-2.

Cohen, Z., Heimer, Y.M., 1990. Δ6 Desaturase inhibition: a novel mode of action of norflurazone. Plant Physiol. 93 (1), 347–349. https://doi.org/10.1104/pp.93.1.347.

Cordero, B.F., Couso, I., Leon, R., Rodriguez, H., Vargas, M.A., 2012. Isolation and characterization of a lycopene ε-cyclase gene of *Chlorella (Chromochloris) zofingiensis*. Regulation of the carotenogenic pathway by nitrogen and light. Mar. Drugs 10, 2069–2088. https://doi.org/10.3390/md10092069.

Cordero, B.F., Couso, I., León, R., Rodríguez, H., Vargas, M.Á., 2011. Enhancement of carotenoids biosynthesis in *Chlamydomonas reinhardtii* by nuclear transformation using a phytoene synthase gene isolated from *Chlorella zofingiensis*. Appl. Microbiol. Biotechnol. 91 (2), 341–351. https://doi.org/10.1007/s00253-011-3262-y.

Couso, I., Vila, M., Vigara, J., Cordero, B.F., Vargas, M.Á., Rodríguez, H., León, R., 2012. Synthesis of carotenoids and regulation of the carotenoid biosynthesis pathway in response to high light stress in the unicellular microalga *Chlamydomonas reinhardtii*. Eur. J. Phycol. 47 (3), 223–232. https://doi.org/10.1080/09670262.2012.692816.

da Silva Ferreira, V., Sant'Anna, C., 2017, Impact of culture conditions on the chlorophyll content of microalgae for biotechnological applications, World J. Microbiol. Biotechnol. https://doi.org/10.1007/s11274-016-2181-6.

DuBois, M., Gilles, K.A., Hamilton, J.K., Rebers, P.A., Smith, F., 1956. Colorimetric method for determination of sugars and related substances. Anal. Chem. 28 (3), 350–356. https://doi.org/10.1021/ac60111a017.

Gimpel, J.A., Henríquez, V., Mayfield, S.P., 2015. In metabolic engineering of eukaryotic microalgae: potential and challenges come with great diversity. Front. Microbiol. 6, 1376. https://doi.org/10.3389/fmicb.2015.01376.

Guschina, I.A., Harwood, J.L., 2013, Algal lipids and their metabolism, in: algae for biofuels and energy. Springer Netherlands, pp. 17–36. https://doi.org/10.1007/978-94-007-5479-9_2.

Huang, W., Lin, Y., He, M., Gong, Y., Huang, J., 2018. Induced high-yield production of zeaxanthin, lutein, and β-carotene by a mutant of *Chlorella zofingiensis*. J. Agric. Food Chem. 66 (4), 891–897. https://doi.org/10.1021/acs.jafc.7b0540010.1021/acs.jafc.7b05400.s001.

Jahns, P., Latowski, D., Strzalka, K., 2009. Mechanism and regulation of the violaxanthin cycle: the role of antenna proteins and membrane lipids. Biochim. Biophys. Acta - Bioenerg. 1787 (1), 3–14. https://doi.org/10.1016/j.bbabio.2008.09.013.

Kim, G., Bae, J., Lee, K., 2016. Nitrate repletion strategy for enhancing lipid production from marine microalga *Tetraselmis* sp. Bioresour. Technol. 205, 274–279. https://doi.org/10.1016/j.biortech.2016.01.045.

Kim, J., DellaPenna, D., 2006. Defining the primary route for lutein synthesis in plants: the role of *Arabidopsis* carotenoid β-ring hydroxylase CYP97A3. Proc. Natl. Acad. Sci. 103, 3474–3479. https://doi.org/10.1073/pnas.0511207103.

Kim, J., Kim, M., Lee, S., Jin, E., 2020. Development of a *Chlorella vulgaris* mutant by chemical mutagenesis as a producer for natural violaxanthin. Algal Res. 46, 101790. https://doi.org/10.1016/j.algal.2020.101790.

Kleinegris, D.M.M., van Es, M.A., Janssen, M., Brandenburg, W.A., Wijffels, R.H., 2010. Carotenoid fluorescence in *Dunaliella salina*. J. Appl. Phycol. 22 (5), 645–649. https://doi.org/10.1007/s10811-010-9505-y.

Li, M., Gan, Z., Cui, Y., Shi, C., Shi, X., 2013. Structure and function characterization of the phytoene desaturase related to the lutein biosynthesis in *Chlorella prototheocoides* CS-41. Mol. Biol. Rep. 40 (4), 3351–3361. https://doi.org/10.1007/s11033-012-2410-5.

Lichtenthaler, H.K., Wellburn, A.R., 1983. Determinations of total carotenoids and chlorophylls a and b of leaf extracts in different solvents. Biochem. Soc. Trans. 11, 591–592. https://doi.org/10.1042/bst0110591.

Lim, D.K.Y., Schuhmann, H., Sharma, K., Schenk, P.M., 2015. Isolation of high-lipid *Tetraselmis suecica* strains following repeated UV-C mutagenesis, FACS, and high-throughput growth selection. BioEnergy Res. 8 (2), 750–759. https://doi.org/10.1007/s12155-014-9553-2.

Lourenço, S.O., Barbarino, E., Lavín, P.L., Lanfer Marquez, U.M., Aidar, E., 2004. Distribution of intracellular nitrogen in marine microalgae: calculation of new nitrogen-to-protein conversion factors. Eur. J. Phycol. 39 (1), 17–32. https://doi.org/10.1080/0967026032000157156.

Ma, R., Zhao, X., Ho, S.-H., Shi, X., Liu, L., Xie, Y., Chen, J., Lu, Y., 2020. Co-production of lutein and fatty acid in microalga *Chlamydomonas* sp. JSC4 in response to different temperatures with gene expression profiles. Algal Res. 47, 101821. https://doi.org/10.1016/j.algal.2020.101821.

Ma, R., Zhao, X., Xie, Y., Ho, S.H., Chen, J., 2019. Enhancing lutein productivity of *Chlamydomonas* sp. via high-intensity light exposure with corresponding carotenogenic genes expression profiles. Bioresour. Technol. 275, 416–420. https://doi.org/10.1016/j.biortech.2018.12.109.

Mendoza, H., de la Jara, A., Freijanes, K., Carmona, L., Ramos, A.A., de Sousa Duarte, V., Serafim Varela, J.C., 2008, Characterization of Dunaliella salina strains by flow cytometry: a new approach to select carotenoid hyperproducing strains. Electron. J. Biotechnol. 11, 1–13. https://doi.org/10.2225/vol11/issue4-fulltext-2.

Michels, M.H.A., Camacho-Rodríguez, J., Vermuë, M.H., Wijffels, R.H., 2014. Effect of cooling in the night on the productivity and biochemical composition of *Tetraselmis suecica*. Algal Res. 6, 145–151. https://doi.org/10.1016/j.algal.2014.11.002.

Moha-León, J.D., Pérez-Legaspi, I.A., Ortega-Clemente, L.A., Rubio-Franchini, I., Ríos-Leal, E., 2019. Improving the lipid content of *Nannochloropsis oculata* by a mutation-selection program using UV radiation and quizalofop. J. Appl. Phycol. 31 (1), 191–199. https://doi.org/10.1007/s10811-018-1568-1.

Mulders, K.J.M., Lamers, P.P., Martens, D.E., Wijffels, R.H., Bassi, R., 2014. Phototrophic pigment production with microalgae: biological constraints and opportunities. J. Phycol. 50 (2), 229–242. https://doi.org/10.1111/jpy.12173.

M. U., N., Mehar, J.G., Mudliar, S.N., Shekh, A.Y., 2019. Recent advances in microalgal bioactives for food, feed, and healthcare Products: commercial potential, market space, and sustainability. Compr. Rev. Food Sci. Food Saf. 18 (6), 1882–1897. https://doi.org/10.1111/crf3.v18.610.1111/1541-4337.12500.

Okuyama, H., Orikasa, Y., Nishida, T., 2008. Significance of antioxidative functions of eicosapentaenoic and docosahexaenoic acids in marine microorganisms. Appl. Environ. Microbiol. 74 (3), 570–574. https://doi.org/10.1128/AEM.02256-07.

Pereira, H., Barreira, L., Figueiredo, F., Custódio, L., Vizetto-Duarte, C., Polo, C., Rešek, E., Aschwin, E., Varela, J., 2012. Polyunsaturated fatty acids of marine macroalgae: potential for nutritional and pharmaceutical applications. Mar. Drugs 10, 1920–1935. https://doi.org/10.3390/md10091920.

Pereira, H., Barreira, L., Mozes, A., Florindo, C., Polo, C., Duarte, C.V., Custódio, L., Varela, J., 2011. Microplate-based high throughput screening procedure for the isolation of lipid-rich marine microalgae. Biotechnol. Biofuels 4 (1), 61. https://doi.org/10.1186/1754-6834-4-61.

Pereira, H., Gangadhar, K.N., Schulze, P.S.C., Santos, T., de Sousa, C.B., Schueler, L.M., Custódio, L., Malcata, F.X., Gouveia, L., Varela, J.C.S., Barreira, L., 2016. Isolation of a euryhaline microalgal strain, *Tetraselmis* sp. CTP4, as a robust feedstock for biodiesel production. Sci. Rep. 6, 35663. https://doi.org/10.1038/srep35663.

Pereira, H., Schulze, P.S.C., Schüler, L.M., Santos, T., Barreira, L., Varela, J., 2018. Fluorescence activated cell-sorting principles and applications in microalgal biotechnology. Algal Res. 30, 113–120. https://doi.org/10.1016/j.algal.2017.12.013.

Pereira, H., Silva, J., Santos, T., Gangadhar, K.N., Raposo, A., Nunes, C., Coimbra, M.A., Gouveia, L., Barreira, L., Varela, J., 2019. Nutritional potential and toxicological evaluation of *Tetraselmis* sp. CTP4 microalgal biomass produced in industrial photobioreactors. Molecules 24, 3192. https://doi.org/10.3390/molecules24173192.

Renaud, S.M., Thinh, L.-V., Lambrinidis, G., Parry, D.L., 2002. Effect of temperature on growth, chemical composition and fatty acid composition of tropical Australian microalgae grown in batch cultures. Aquaculture 211 (1-4), 195–214. https://doi.org/10.1016/S0044-8486(01)00875-4.

Schüler, L., Greque de Morais, E., Trovão, M., Machado, A., Carvalho, B., Carneiro, M., Maia, I., Soares, M., Duarte, P., Barros, A., Pereira, H., Silva, J., Varela, J., 2020a. Isolation and characterization of novel *Chlorella vulgaris* mutants with low chlorophyll and improved protein contents for food applications. Front. Bioeng. Biotechnol. 8, 1–10. https://doi.org/10.3389/fbioe.2020.00469.

Schüler, L.M., Santos, T., Pereira, H., Duarte, P., Katkam, N.G., Florindo, C., Schulze, P.S.C., Barreira, L., Varela, J.C.S., 2020b. Improved production of lutein and β-carotene by thermal and light intensity upshifts in the marine microalga *Tetraselmis* sp. CTP4. Algal Res. 45, 101732. https://doi.org/10.1016/j.algal.2019.101732.

Schulze, P.S.C., Carvalho, C.F.M., Pereira, H., Gangadhar, K.N., Schüler, L.M., Santos, T. F., Varela, J.C.S., Barreira, L., 2017. Urban wastewater treatment by *Tetraselmis* sp. CTP4 (Chlorophyta). Bioresour. Technol. 223, 175–183. https://doi.org/10.1016/j.biortech.2016.10.027.

Shin, H., Hong, S.J., Yoo, C., Han, M.A., Lee, H., Choi, H.K., Cho, S., Lee, C.G., Cho, B.K., 2016. Genome-wide transcriptome analysis revealed organelle specific responses to temperature variations in algae. Sci. Rep. 6, 1–11. https://doi.org/10.1038/srep37770.

Steinbrenner, J., Linden, H., 2003. Light induction of carotenoid biosynthesis genes in the green alga *Haematococcus pluvialis*: regulation by photosynthetic redox control. Plant Mol. Biol. 52, 343–356. https://doi.org/10.1023/A:1023948929665.

Varela, J.C., Pereira, H., Vila, M., León, R., 2015. Production of carotenoids by microalgae: achievements and challenges. Photosynth. Res. 125 (3), 423–436. https://doi.org/10.1007/s11120-015-0149-2.

Zhao, Y., Wang, H.-P., Han, B., Yu, X., 2019. Coupling of abiotic stresses and phytohormones for the production of lipids and high-value by-products by microalgae: a review. Bioresour. Technol. 274, 549–556. https://doi.org/10.1016/j.biortech.2018.12.030.